COMPOSITION ANALYSIS OF STRONGLY OXIDIZED Nb_3Ge WITH X. P. S.

Tetsuya ŌGUSHI, Yoshihisa ŌSONO and Tadashi NUMATA

(Received May 31, 1986)

ABSTRACT

A new candidatite for superconductor is introduced as the results of our recent studies on the fabrication and properties of a strongly oxidized Nb_3Ge thin film prepared on a Al_2O_3–substrate. These experiments were triggered by our investigation to improve the reproducibility of the resistance anomaly of Nb–Si thin films reprorted earlier by us.

The new films are confirmed to have resistance transition at a temperature of 44.5K along with a large diamagnetic transition. They also has good reproducibility and stability. A substantial amount of Al and O exisis in the film resulting in the formation of Nb_2O_5, GeO_2 and Al_2O_3 through strong oxidation. The chief characteristics of this transition are notably similar to superconductors with phonon–mediated electron–electron interaction. To explain the high T_C, however, we might have to consider another mechanism (i. e excitonic mechanism), which acknowledge the possibility of high–temperature carrier pairing.

1. INTRODUCTION

The pursuit for material with high superconducting critical temperature has been an area of intense research. In 1973 Gavalar[1] sputtered Nb–Ge films in high Argon pressure onto hot substrates and obtained superconducting transitions with an onset temperature (T_{CO}) of 22.3K. Soon after, Testardi[2] achieved $T_{CO} = 23.2$K using the same material. Many researchers have extensively examined Nb_3Ge . The T_{CO} for this compound has not exceeded 23.9K[3] until now.

Dew–Hughes[4] predicted from the empirical relationship for the critical temperature of some A15 superconductors, that if Nb_3Si crystallizes in the A15 structure, it should have $T_C \simeq 38$K. However, crystal in a good ordered state with a small lattice constant is very difficult to make. Geller[5] also has suggested a stoichiometric β–W type Nb_3Si should have a superconducting transition temperature between 31K and 35K. Many experimental[6~16] have been attempted to obtain a smaller lattice constant of ~ 5.09Å with A15 phase to achieve a high T_C. Although the lattice constant and phase were realized, the T_C for Nb_3Si never exceeded 18.6K.

Recently, many theories have been proposed for a high temperature superconductor from electron–electron interaction via exchange of nonphonon[17 ~ 21] . In particular, Allender, Bray and Bardeen[18] have discussed in detail the possibility of using a narrow–gap semfconductor as a suitable medium for an exciton mechanism superconductor. In their theory they discussed the possibility of ex-

---

Note added for proof

An accurate measurement of the transition temperature is now being examined.

citon mechanism and phonon mechanism working together. It seems quite interesting from an experimental point of view because superconductors from phonon–mediated electron–electron interaction such as Nb_3Si and Nb_3Ge could be converted to that state with both the exciton mechanism and the phonon mechanism.

One of the authors of this manuscript has reported a resistance anomaly of very thin Nb–Si film[22]. The anomaly is marked by a sudden drop in the resistance by a factor of $\sim 10^3$ at a temperature of $\sim$ 180K. This behavior bears many resemblances to that of a superconductor. However, the accuracy of measurements had been hampered by poor reproducibility of the anomaly. Recently, it became apparent to us that the presence of oxygen during sputtering remarkably improved the reproducibility of the resistance anomaly and therefore promoted the oxidation of Nb_3Ge where Ge is substituted for Si in the Nb–Si film.

Artificially oxidized films were examined, but the characteristics underwent changes every hour and were also affected by thermal cycles. Therefore, Nb_3Ge films with $T_{CO}=21\sim22$K prepared one$\sim$four years ago and thus, naturaly oxidized in air , have been examined.

In this paper we will demonstrate, as testimony for their candidacy for superconductor, the resistive transition and diamagnetic behavior of the Nb_3Ge films oxidized naturaly. Results of X–ray and the data from X–ray photoelectron spectroscopy analysis (X.P.S) are also presented.

The mechanism of this superconductor has not yet been clarified. However, it has emphatically different characteristics from "an ordinary superconductor". For example, light sensitivity, X–ray irradiation–sensitivity and large hysteresis ($\sim$9K in maximum) between a cooling and warming process have been observed. These phenomena would not be explained by a phonon–mechanism–superconductivity.

II. EXPERIMENTS

A. Sample Preparation

Sample were prepared by the following methods:

[1] Nb and Ge were sputtered onto a heated substrate in highly pure Ar with a controlled slow of oxygen into the chamber.

[2]After preparing Nb_3Ge with high T_C by a sputtering process, they were oxidized in a pure oxygen atmosphere.

[3] Nb_3Ge was naturally oxidized in air for 1$\sim$4 years.

The samples obtained by the first two methods showed a lack of stability, and characteristics changed with time. The results obtained by these two methods will be published elsewhere.

All samples reported here were prepared by method [3] where the D.C. high–rate sputtering carried out in a can cooled by liquid N_2. All films were deposited onto polished single–crystal sapphire substrates $15\times10\times1.0$mm in size. The thickness of the films were 3000Å$\sim$5000Å. The details have been described by Ōgushi et al[23].

B. Method of Measurement

The transition temperature was measured by using an Au–0.07%Fe versus chromel thermocouple calibrated with GaAs diode standard (Lake shore Corp.) and with the boiling temperature of liquid N_2 and He. The thermocouple was held tightly to the samples. A digital voltmeter was used to read the voltage of the thermocouple with an accuracy of five digits. Periodically to confirm the accuracy of our measurements the samples were cooled or warmed very carefully and slowly at the rate of 1K/

min. A metal Dewar with a dark interior for liquid–He was used to cool samples. Periodically, a glass Dewar was used instead to introduce light.

The inductive measurements were carried out with a helical coil followed by a pick up coil of the same type which was in direct contact with the sample to measured. Duplicate pairs of coils were utilized to prevent sprious signal detection. Normally, the frequency of the driving coil was 88C/sec with frequent changes from 88C/sec to 10C/sec. To observe the effect of eddy current, a pure Nb foil with much higher conductivity than the films were examined for all frequency used here. However, no signal except those attributed to the real superconductive transition was detected.

The magnetic field–strength of the driving coil was purposely chosen to be low as not to induce vortex penetration through a thin film. The signal from the Nb foil was then used for calibration of absolute values and sighns of susceptibility.

C. Transition Measurement

A quasi four–terminal–method in which pure gold wires are contacted with pressure to films was used. These measurements were verified at intervals by the use of typical four terminal method to insure uniformity of current necessary for accurate measurements. Both methods were sound to coincide. The measuring current was normally $10\mu A$ but sometimes $20\mu A$ was used to observe current dependency.

Fig. 1 shows a photocopy of X–Y recorder trace of a resistive transition curve for the sample X–457. The dotted line represents the diamagnetic susceptibility (χ) which was transcribed from a X–Y recorder trace. The T_{CO} of the transition of this film is 44.5K which was the highest detected in our experiments. The diamagnetic trace increases towards a plus porality maximum of 0.4, crossing the absissa and goes toward the minimum of $X = -0.92$. The diamagnetism trace decrease inversely with the resistance. The temperature at which the resistance reaches it's half value (T_C) is 34.0K. But

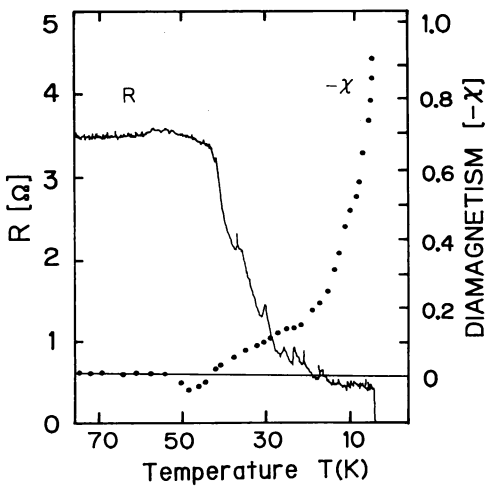

Fig. 1 Resistive transistion curve (solid line) and the accompanied diamagnetic susceptibility (χ) for sample χ for sample χ 457.T_{co}= 44.5K and $\chi = -0.92$ at the maximum (in the cooling course).

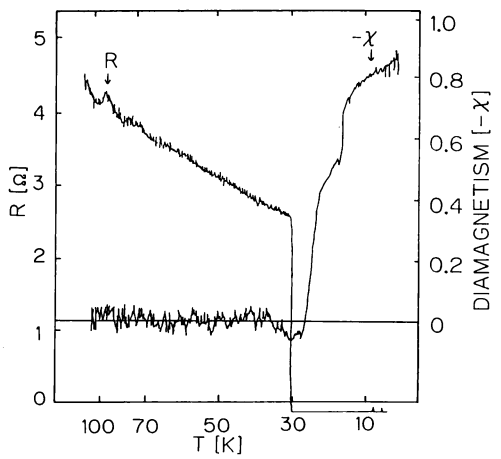

Fig. 2 Same trace in the cooling course for sample YH 8001–16 as in Fig. 1 (T_{co} = 30.5, T_c = 30.0, T_{ce} = 29.5K). T_{ce} represents a temperature at which a resistance becomes zero.

the resistance remains finite until 7.5K.

In Fig. 2, a sharp transition for sample YH 8001−16 is demonstrated. The transition temperature are $T_{CO}=30.5K$, $T_C=29.5K$ and $T_{Ce}=29.5K$. The T_{ce} is the temperature at which a resistance becomes zero. Unexpectedly. the trace declined to minus resistance in most samples particularly in those with the sharp transition. This is ascribed to a complex electromotive force (EMF), the amplitude of which is partly dependent on temperature and is quite noisy;

The typical EMF and temperature for sample X 330−Ⅱ is shown in Fig.3. It attains maximum

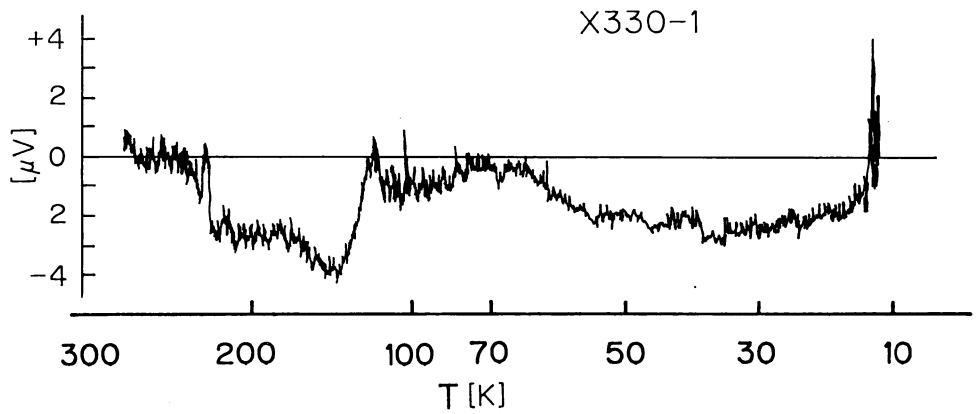

Fig. 3 Typical "zero bias voltage" induced between terminals for a measurement of a resistance. This voltage is super imposed on an ordinary R−T curve. A noisy trace of R is due to voltage. A polarity of this voltage usualy changes from (−) to (+) polarity below T_{ce}. This leads to a false residual resistance (in the course of cooling).

Table 1

Sample No.	T (REDUCTION) (K)			T (RAISE) (K)		
	Ton	Tc	Tce	Ton	Tc	Tce
X 457	44.5	34.0	7.5	22.0	12.5	7.5
Y H 8001−16	30.5	30.0	29.5	25.0	24.0	22.5
X 279	37.0	36.0	33.5	24.5	23.5	21.2
X 277	32.5	32.0	30.0	26.0	24.0	20.0
(＊) X 2770	39.5	36.5	9.5	24.5	22.5	9.5
X 100	35.0	34.0	−	26.0	24.5	15.0
X 308	34.0	32.5	30.5	25.0	21.9	20.0
(＊) X 309	25.1	7.5	−	18.5	8.4	−
X 324−	29.5	26.8	−	21.4	17.1	−
X 326	33.0	32.8	23.5	23.5	23.9	12.8
X 280	31.2	29.3	25.0	23.79	20.1	19.5
X 310	34.8	31.6	29.8	25.6	21.5	20.1
X 332− I	33.5	33.0	−	24.5	24.6	19.0
X 330− I I	32.3	30.4	29.2	21.3	19.0	−
X 330	33.1	32.4	32.3	24.3	22.6	20.0
X 331	37.5	37.5	37.5	25.0	23.0	21.0
(＃) X 331	37.5	37.5	37.5	37.5	37.5	37.5

and minimum (±) 4μV. When this EMF signal is superimposed on an ordinary R–T curve, the results is an R–T curve similar to that shown in Fig. 2. This addition signal can not be ignored because the measuring currents of film resistance is usually 10μA, which induces, for example, 40μV between voltage terminals of a sample with 4 Ω in the resistance. The noisy characteristic of R–T curve is, therefore, presumably due to this EMF.

In Table I, T_{CO}, T_C and T_{Ce} in both the cooling and warming processes are listed. The hysteresis is described below.

D. Hysteresis

Plots of a resistance vs the temperature have a hysteresis loop for the thermal–cycle. This hysteresis is not so simple. The distortions in shape of the hysteresis loop are determined by the starting temperature of cooling and warming a sample in the thermal–cycle.

The traces of resistive transition together with the diamagnetic in which the sample X 280 was cooled from room temperature is shown in Fig. 4. The minor hysteresis loops for the same samples are shown in Fig. 5. The trace with numbered 1 was cooled from 77K to 22.5K and then warmed up to 34.0K (No.1'). The trace (No.2,2') is for the thermal cycle from 34.0K down to 13.6K and then from 13.6K up to 28.0K. The trace (No,3,3') represents a similar thermal cycle 28.0K down to 5.0K and then from 5K the temperature was raised.

The quantitative analysis was carried out on sample X 332 (Fig. 6) having the largest observed hysteresis in this study. The results are plotted on semilog graph paper in Fig. 7. The dashed line represents T_{CO} obtained in the cooling process of the film from room temperature. The solid line signifies T_{CO} in the process of warming the sample immediately after cooling the sample always from a room temperature to various T on a horizontal– coordinate axis. The difference between the two lines represents the hysteresis at a corresponding temperature. The linear dependence of $\ln T_{CO}$ on T in the warming process is quite implicating.

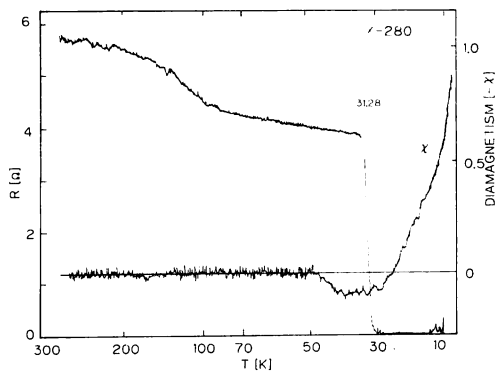

Fig. 4 R–T and the diamagnetism for sample X 280 is shown. The temperature of the sample was decreased from a room temperature. This is shown to the help an explanation of a characteristics in thermal cycles.

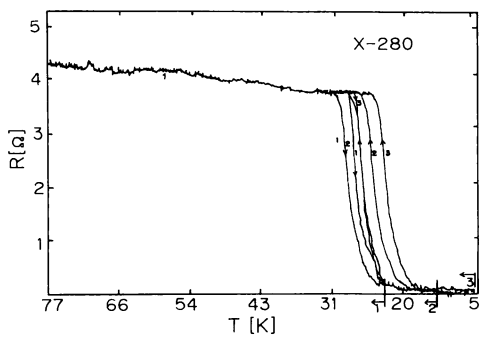

Fig. 5 Minor hysteresis for thermal cycles. Transition temperatures in the course of cooling or warming change depending on what temperature is the starts of thermal cycles.

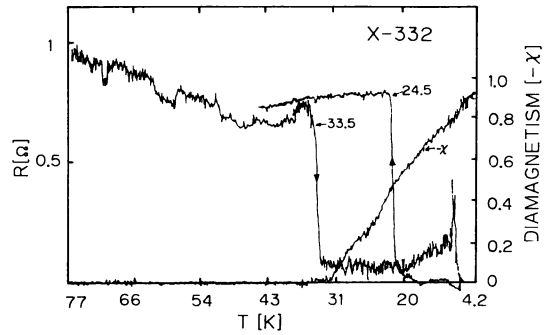

Fig. 6 Quantitative analysis of the hysteresis was carried out for the sample X 332.

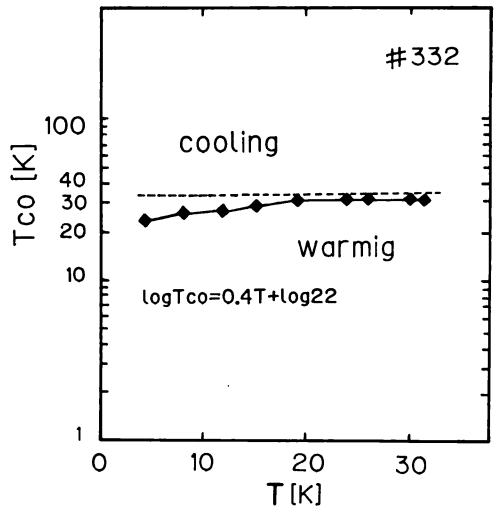

Fig. 7 Temperature dependence of hysteresis loops for the sample X 332. The sample was cooled exactly from room temperature. The transition temperature is represented by a dashed curve. A curve labeled (◆) shows T_{co} in the course of warming but for the temperature T until which the sample was cooled from a room temperature. The critical temperatures for as deposited Nb_3Ge were $T_{co}=22.1$, $T_c=21.3$ and $T_{ce}=16.3X$.

E. X−rav Diffraction Results

Fig. 8 shows the X−ray scan for sample X 277, with a transition temperature of 39.0K. Eight Al5 peaks were observed up to $2\theta=90°$.

These peaks gives a lattice constant (a_0) of 5.124Å. This lattice constant is less than the smallest $a_0=5.13$Å reported for deposited Nb_3Ge films. This scan is characteristic of samples studied in this report. The scan for sample X 309 is so sharp than it shows definite $K_{\alpha 1}-K_{\alpha 2}$ splitting. The both lattice−constants obtained from $K_{\alpha 1}$ and $K_{\alpha 2}$ concide with $a_0=5.110$Å. As is shown later, these films contain a large amount of Al. An unsolved problem is what kind of matrix results in such small lattice constant and good ordered state as will be discussed later.

F. X−ray Photoelectron Spectroscopy

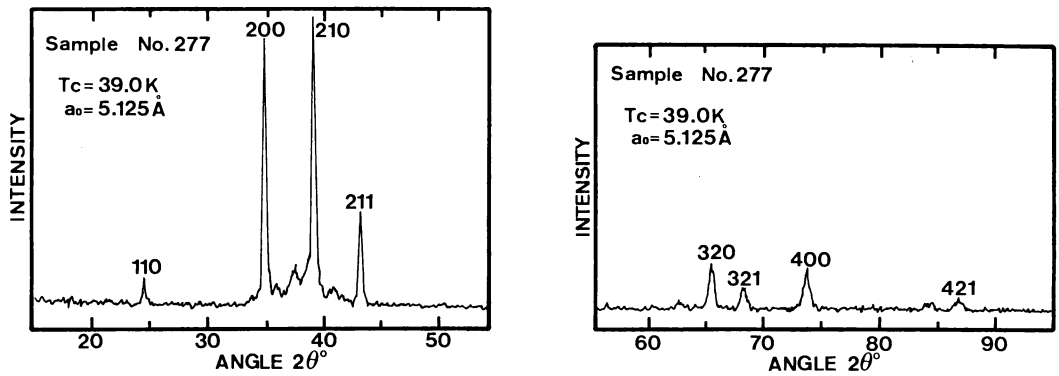

Fig. 8 X-ray trace for sample X 277.

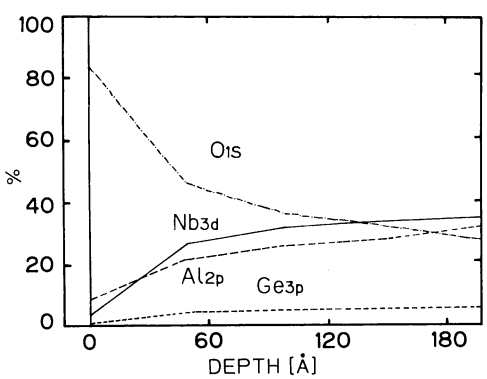

Fig. 9 XPS-depth profile for a sample X-10-B with high critical temperature.

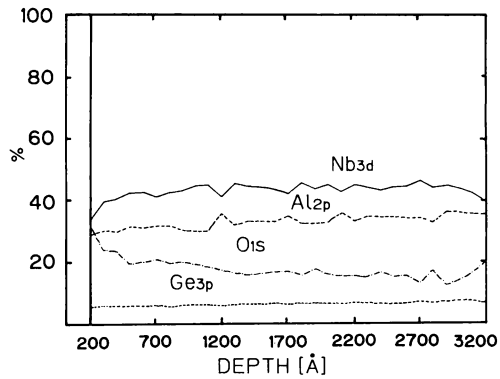

Fig. 10 XPS-depth profile. The film thickness was 3200Å

(a) Composition analysis

X-ray photoelectron Spectroscopy (XPS or ESCA) is a very powerful tool in the study of binding energy of core electron in atoms and molecules. The chemical shifts (ΔE_B) of an individual element have been correlated with the it's binding state in various compounds.

The composition analysis was carried out by XPS. A depth profile (Fig. 9) of a sample X-10-E shows the existence of large quantity of Oxygen (~85% at the surface), Nb, Al and Ge which are in the form Nb_2O_5, Nb_2O, NbO,Al_2O_3 and GeO_2 to the depth of 50Å, identified by the oxide shifts for the various elements[24~27]. Even at the depth 50Å~200Å, the chemical shift from the base metals by oxidation are still observed. The carbon contamination signal was used for the charge-up-compensation. The binding energy of a pure Nb was estimated, and was in good agreement with that obtained by Karulkar et al[24]. and a measurement of a Nb with four-nine-purity. The standard for Al are from Ref. 28.

Fig. 10 is depth profiles between 200Å and 3200Å. and Fig. 10 is that between 3200Å and 5700Å. These profiles are markedly different from of deposited Nb_3Ge[15] since about 30%Al_{2p} and 18%O_{1S} are contained in the main part (200Å ~ 3200Å) of the film. As mentioned before, the film thickness is 3200Å, estimated from multiple-beam interferometry. The distribution of O_{1S} seems to form part of a exponential curve from the surface to the interface between the film and the substrate

(Fig. 9 and 10). This shows that Oxygen has diffused into the film from the surface. It is well know that oxide layer of Nb or Al work as a protective stable layer against the progress of oxidization of metals.

The large amount of Oxygen in films studied in the present research is caused, in our conjecture, by a channel formed by a poorly defined oxides because of the existence of complex elements such as Nb, Ge and Al.

On the other hand, the mechanism proposed by Ihara et al[25] to explain the enrichment of Nb atoms in surface region of Nb_3Ge may also explain the uniform distribution of Al in the region of 200Å~3200Å.

The Nb–Ge atomic ratio increases to 5.5 from 3.0 which was estimated from as–deposited Nb_3Ge by peak–intensity ratio of the Nb_{3d} to Ge_{3p}. This ratio will be represented by Nb_3Ge_{1-X}.

It is impossible to determined, at the present stage of our studies, which additional elements contribute to the Al5 structure and very small lattice–constant as determined by X–ray analysis.

Fig. 11 shows that a large amount of Nb_{3d} has diffused into the sapphire substrate up to ~4700Å through the interface between the film and the sapphire substrate. On the contrary, the peak intensity of Al including Al_{2p} and Al_{2s} evidently decrease [Fig. 14 and 15 (b)]. This means that a exchange diffusion of Nb and Al has occurred on both sides of the interface. The Al librated from Al_2O_3, in our

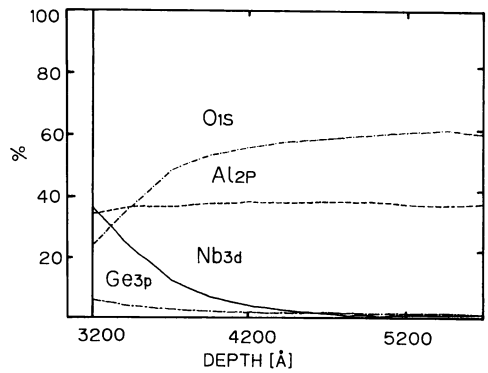

Fig. 11 XPS–depth profile.

opinion, is the source of Al contained in the films. This pattern of compositions–distribution can easily be imagined to depend on the orientation of the sapphire surface.

In our experiment, a surface of a sapphire which makes an angle of 90±7°C to C axis is used as the substrate. This results in a facilitated reaction at the interface..

The reaction of Nb alloy with Al_2O_3 has discussed more extensively Schmid et al.[29]. They prepared Nb_3Al with a transition temperature $\geq$17K by sputtering Nb onto a hot substrate. Nb metal reduces the Al_2O_3 released Al through the formation of Nb_3Al despite Nb's lower Oxygen affinity than Al. The Rutherford back scattering results indicate a fairly uniform Al concentration throughout the film. This seems to coincide with our results.

(b) Binding state

Fig.12 (a) shows the binding energy spectrum of Nb_{3d} of Nb_3Ge. The binding energy of Nb–$3d_{5/2}$ peak and Nb–$3d_{3/2}$ peak are 200.8eV and 203.6eV respectively, after charge up compensation, between the film thickness 400Å and 3200Å. Thses values are lower by 1.5eV than that obtained by

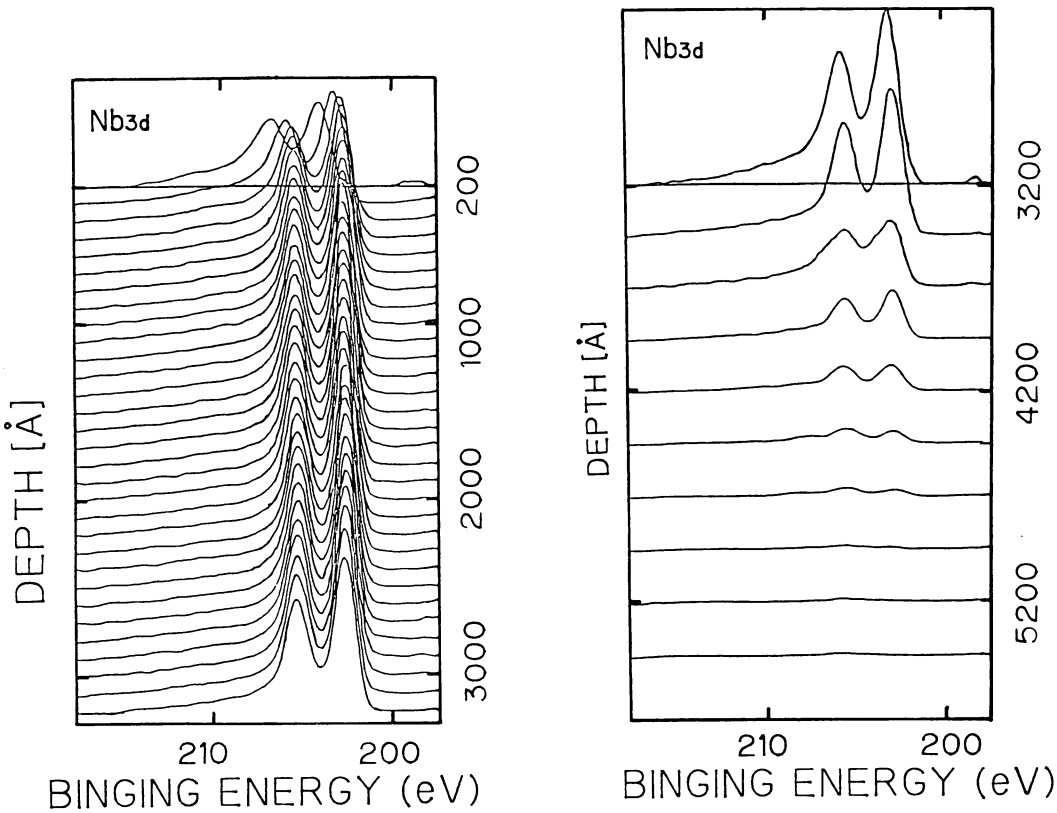

(a) Nb–3d XPS spectra taken from sample X–10–B.

(b) Nb–3d XPS spectra at the depth between 3200Å and 5250Å.

Fig. 12

Ihara et al. from a stoichiometric Nb_3Ge[25]. This suggests together with the composition ratio, that the films studied in this report are not simple Nb_3Ge. Another possibility is the formation of Nb_3Al or $Nb_3(Al_{1-X}Ge_X)$ as a part of a film.

The results on Nb3d are summarized in Fig. 13. The chemical shifts near the surface (0～300Å) show the exsistence of Nb_2O_5, NbO_2 and NbO. The binding energies Nb–$3d_{5/2}$ and Nb–$3d_{3/2}$ are constant from 300Å to the depth ～3200Å which corresponds to the film thickness. ΔE_B～0.3eV of binding energy of Nb–$3d_{3/2}$ appear at the interface where a reaction with the substrate is expected.

XPS spectra for Ge–3d is shown in Fig. 14. The corresponding binding energy is 121.0eV which matches the results of Ge–3p.[25].

Fig. 15 is that for Al–2p. The observed binding energy is ～76.5eV in the core of the film. This also shifts toward a greater binding energy by 1.5eV at the interface reaching that of a sapphire (78.0eV). A calibration for a charge–up has not been done in a sapphire substrate which results in the large ΔE_B.

The observed value Al–2p is higher than that of pure Al suggesting that Al has made a compound with another element. A large amount of Al has been found in the film as demonstrated in Fig. 10

Even if we assume that Nb_3Al is formed instead of the other possibilities of $(NbAl)_3Ge$ or $Nb_3(Al,$

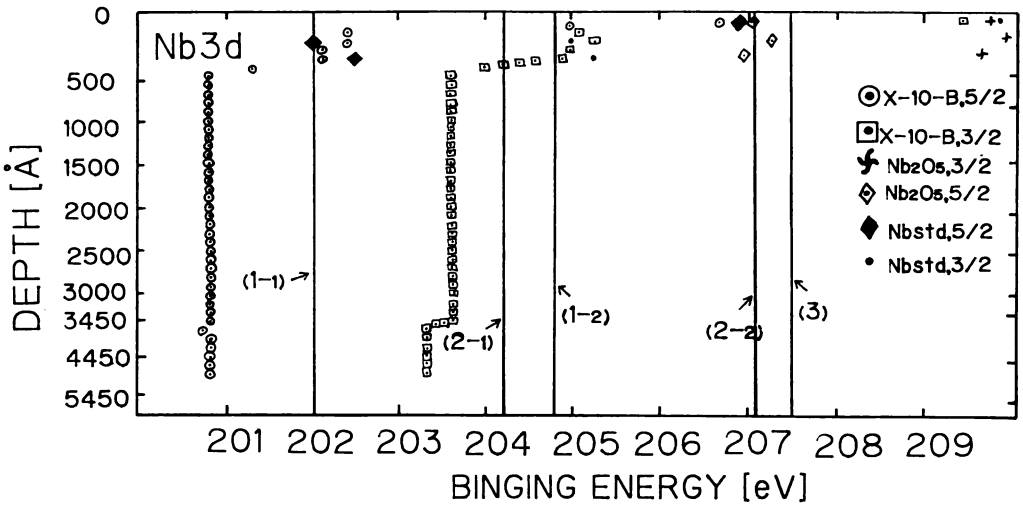

Fig. 13 The result obtained in Fig. 12 are summarized.

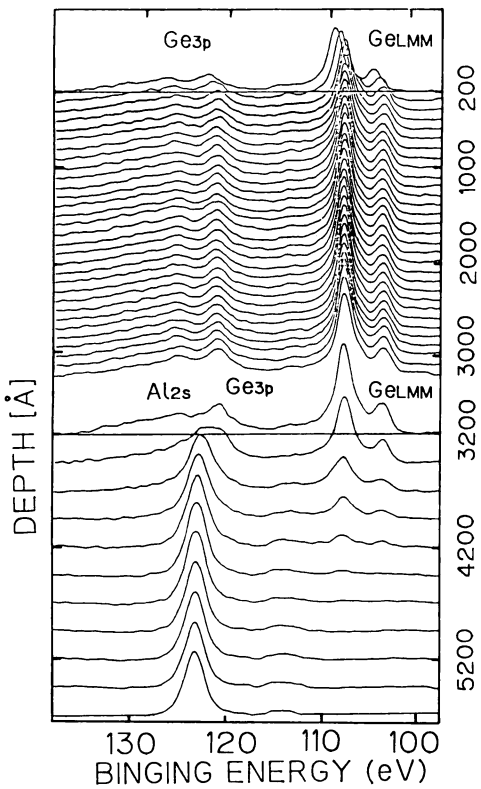

Fig. 14 Ge-3p XPS spectra taken from sample X-10-B.

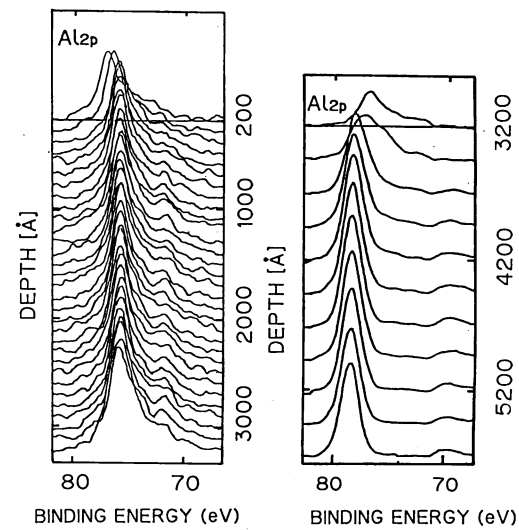

Fig. 15 Al-2p XPS spectra for X-10-B.

Ge)[30] the homogenous niobium chain of which is shorter than Nb_3Al[31], there still remains a surplus of Al.

Aside from problems oxides in the film were examined because ~18% Oxygen had been detected (Fig. 10). The results from the XPS spectra of Nb, Ge and Al can not verify the existence of the oxides of each metal.

Therefore, the XPS spectra of O_{1S} was investigated. The results are shown in Fig.17. Vertical lines with marks Al_2O_3 and GeO_2 indicate binding eoergies of O_{1S} in Al_2O_3 and GeO_2. Symbols (△)and (◇) represent the measurements of standard Nb_2O_5 and SiO. Symbol (○) denotes the experimental.

These data have poven the existence of oxides such as Al_2O_3, Al_2O_X. GeO_2 and Nb_2O_5 even in the matrix of Al5 phase or in the grain boundary of the film.

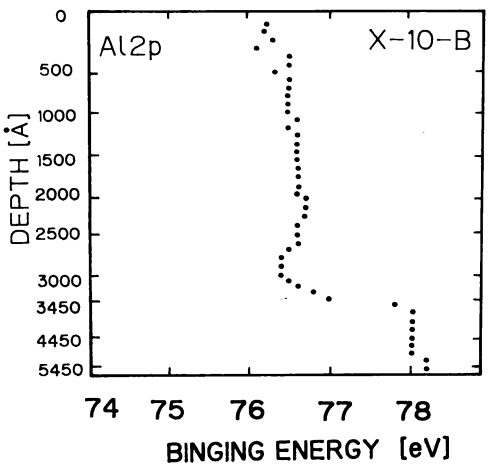

Fig. 16 The results from Fig. 15 are summarized.

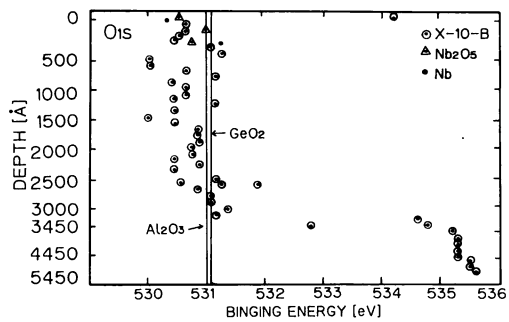

Fig. 17 O-1S XPS spectra are summarized for X-10-B (oxydized Nb_3Ge). This veryfy that the existence of complex oxide such as Al_2O_3, GeO_2, Nb_2O_5 in the matrix or in grain boundary of the film.

III. DISCUSSION

We consider the transition reported here a superconductive one due to the associated large diamagnetism and a current-induced-transition by $\sim 2\times10^{-6}$A at 4.2K (not mentioned in this report).

It has became clear that a Nb_3Ge , which contains a large amount of Oxygen results in the formation of oxides such as Nb_2O_5, NbO_2, GeO_2, Al_2O_3 and Al_2O_X leading to a susptantially enhanced transition temperature. The better the qualities the deposited Nb_3Ge has, the higher the T_{CO} and the sharper the transition it will bring about, after oxidation. In our experiments, Nb_3Ge with T_{CO} less than 19K has not shown any increased transition -temperatures. Our results demonstrate that this spectracular jump of superconductive transition temperature are undoubtedly related to the mechanism of an ordinary superconductor.

The Al5 strcture, however, even with the $a_0 \sim 5.125$ or 5.110Å obtained by us, could not have a T_{CO} as high as 44.5K. Furthermore, the superconducting characteristics are remarkably different from that of an ordinary superconductor. The first example is the existence of a large hysteresis loop in a resistive transition-characteristic caused by thermal cycles. The typical one for sample X332 is shown in Fig. 6. As is explained in Ⅱ-D, the transition temperatures T_{CO} s in warming process depend on the lowest end of temperature in the thermal cycles, the higher returning-temperatures of the cycles were fixed always to a room temperature. The horizontal coordinate axis shows the lowest

end of temperature in the cycles. The vertical axis indicate correlative T_{CO} to the lowest temperatures (returning ones) in the warming process. In this same manner, the solid line in Fig. 7 was plotted. The T_{CO} obtained in cooling process exactly from a room temperature is shown by a dashed line. The solid line is represented by log $T_{CO}=0.4T+\log 22$ below 19K. We think that the enhancement of the critical temperature (α) discussed by another mechanism (such as excitonic mechanism) which depends on temperature and has a slope of 0.4T on as shown in Fig. 7. 22K is the critical temprature of an ordinary superconductor. α staturates at the temperature 19K results in a disappearance of the hysteresis. We note in parenthesis that T_{CO} of as deposited thin film was 22.1K in good agreement with T_{CO} at $T=0$ in the above equation.

A second example is sensitivity to light. The hysteresis was observed only when the measurement was carried out in a metal Dewar which has a dark interior. The hysteresis disappeared in a transparent glass Dewar.

The third evidence is that the R in R–T curve is very noisy. The very noisy zero–bias voltage such as shown in Fig. 3 is superimposed on an ordinary one. The voltage mainly is due to thermoelectricity. A small amount of noise, however, is thought to be caused by piezoelectricity induced by a strain between a film and a substrate. Samples with high T_C and a sharp transition have a tendency to have large voltage. We have not observed to date such voltage in the measurement for as–deposited Nb_3Ge.

The presence of Oxygen has been shown to be essential. A composition analysition analysis has verified that Al_2O_3, Al_2O_X, GeO_2, Nb_2O_5 and Nb_2 are contained in the matrix and probably in the boundary of grains. These oxides are a semiconductor or an insulator the energy gap of which are, respectivily, Al_2O_3 ~7eV, Al_2O_X——, GeO_2 ~5,16eV, Nb_2O_5 ~1eV and NbO_2 ~0.66eV. These evidences seems to be explained by the excitonic model proposed by A. B. B.

An X–ray peak corresponding to Al can not be found in the X–ray trace despite the large amount of the illustrated Al. The composition analysis by Ion Micro Analyzer (IMA) shows that the quantity of Al in the films is about10%. These results are accepted as reasonable for our circumstances. We suspect that the quantity of Al shown in Fig. 9 and 10 includes the contribution from the Auger electron of Ge At 77eV. Therefore, the net quantity of Al is arrived at substracting this from the value shown in Fig.10.

In summary, a superconductor with a maximum transition temperature of 44.5K has been realized through strong oxidation of high quality Nb_3Ge. The Al5 structure of Nb_3Ge but with a smaller lattice constant has been confirmed to remain. The complex oxides have been formed in the film by the process mentioned above. It seems to provide the large increment of T_{CO} over a temperature range of 20K above a T_{CO} ~24K of Nb_3Ge. A.B.B. had given calculations with enough detail using realistic parameters to estimate transition temperature for the exciton and phonon mechanism acting simultaneously. However, until more experiments are done to see if the present results come from the excitonic mechanism, the final decision must remain open.

Acknowledgements

The authors wish to acknowledge their grateful thanks to professor T. Geballe for his interest and encouragement. Thanks are also due to professors T. Anayama, Y. Shibuya and H. Fukuyama for their suggestions and discussions. The authors are indebted for their technical assistance to Messrs. K. Obara, T. Watanabe, M. Yuda, H. Nagai, Y. Kaneko and K. Azuma.

The present work was supported partly by a Grant–in–Aid for Scitentific Reseach of Ministry

of Education.

REFERENCES

1) J. R. Gavalar, Appl. Phys. Lett. 23, 480 (1973).
2) L. R. Testardi, Solid State Commun.15, 1 (1974).
3) A. I. Golovashkin, E. V. Pechen, A. I. Skvortsov nand N. E. Khlebova, Sov. Phys. Solid State, 23, 774 (1981).
4) D. Dew–Hughes and V. G. Rivlin, 250, 723 (1974).
5) S. Geller, Appl. Phys.,7, 321 (1975).
6) V. F. Pan, V. P. Alekseevski, A. G. Popov, Y. I. Beletski, L. M. Yupko and V. V. Varosh, JETP Lett., 21, 288 (1975).
7) D. Dew–Huges and V. D. Lides, J. Appl. Phys.,50, 3500(1979).
8) R. M. Waterstrat, F. Haenssler and J. Müller, J. Appl. Phys., 50. 4763 (1973).
9) R. D. Feldman, R. H. Hammond and T. E. Geball, Appl. Phys. Lett., 35, 818 (1979).
10) R. M. Waterstrat, F. Haenssler, J. Müller, S. D. Dahlgren and J. O. Willis, J. Appl. Phys. 49, 1143 (1978).
11) R. E. Someck and J. E. Evett, IEEE Trans. Magn.,15, 194 (1979).
12) M. T. Clapp and R. M. Rose ,Appl. Phys. Lett.,33, 205 (1978).
13) H. Kawamura and K. Tachikawa, Phys. Lett., A55, 65 (1975).
14) L. R. Testardi, T. Wakiyama and W. A. Royer, J. Appl. Phys., 43, 2055 (1977).
15) T. Ōgushi, K. Nishi, H. Nagai, K. Obara and T. Numata, J. Low Temp. Phys.,41(1/2), 13 (1980).
16) Bart Olinger and L. R. Newkirk, Solid State Commun.,37, 613 (1981).
17) Bart Olinger and L. R. Newkirk, Solid State Commun., 37, 613 (1981).
17) W. A. Little, Phys. Rev., B4A, 1416 (1964).
18) D. Allender, J. Bray and J. Bardeen, Phys. Rev.,B7, 1020 (1973).
19) A.A. Abrikosov, JETP Lett.,27, 219 (1978).
20) A. Fukuyama, J. Phys. Soc. Jpn.,51, 1709 (1982).
21) M. Grabowski and L. J. Sham, Phys. Rev.B, 29, 6132 (1984).
22) T. Ōgushi, K. Obara and T. Anayama, Jpn. J. Appl. Phys., 22, L523 (1983).
23) T. Ōgushi, T. Watanabe, M. Yuda, Y. Kaneko, Y. Hakuraku and T. Numata, Jpn. J. Appl. Phys.,19, 2003 (1980).
24) Pramod C. Karulkar and J. E. Nordman, J. Vac. Sci Tech.,17, 462 (1980).
25) H. Ihara, Y. Kimura, M. Yamazaki and S. Gonda, Phys. Rev. B27, 551 (1983).
26) L. Lindau and W. E. Spicer, J. Appl. pPhys., 45, 3720 (1974).
27) R. Holm and S. Storp, Appl. Phys.,9, 217 (1976).
28) Shimazu Application News, No.4.
29) P. H. Schmid, J. M. Rowell and W. L. Feldman.,Appl. Phys.Lett.,39, 177 (1981).
30) N. V. Ageev, N. E. Alekseevskii and V. F. Shamray, Phys. Stat. Sol. (b)77, K 129 (1976).
31) F. Y. Franklin, C. Y. Wang, C. H. Lin, Y. H. Kao and C. P. Khattak, J. Less. Comm. Metals, 71, 47 (1980).
32) Y. Kaneko and Y. Suginohara, nihon Kinzoku Gakkaishi, 41, 375 (1977).